Neoplasia • Vol. 7, No. 4, April 2005, pp. 356–368 356

www.neoplasia.com

mTOR Promotes Survival and Astrocytic Characteristics Induced by Pten/Akt Signaling in Glioblastoma[1]

*Xiaoyi Hu**, Pier Paolo Pandolfi**, Yi Li*[†], Jason A. Koutcher*[‡], Marc Rosenblum*[§] and Eric C. Holland,**[,¶]

*Department of Cancer Biology and Genetics, Memorial Sloan-Kettering Cancer Center, New York, NY, USA; [†]Department of Molecular and Cellular Biology, Baylor College of Medicine, Houston, TX, USA; Departments of [‡]Radiology, [§]Pathology and [¶]Surgery (Neurosurgery) and Neurology, Memorial Sloan-Kettering Cancer Center, New York, NY, USA

Abstract

Combined activation of Ras and Akt leads to the formation of astrocytic glioblastoma multiforme (GBM) in mice. In human GBMs, *AKT* is not mutated but is activated in approximately 70% of these tumors, in association with loss of PTEN and/or activation of receptor tyrosine kinases. Mechanistic justification for the therapeutic blockade of targets downstream of AKT, such as mTOR, in these cancers requires demonstration that the oncogenic effect of PTEN loss is through elevated AKT activity. We demonstrate here that loss of Pten is similar to Akt activation in the context of glioma formation in mice. We further delineate the role of mTOR activity downstream of Akt in the maintenance of *Akt+KRas*–induced GBMs. Blockade of mTOR results in regional apoptosis in these tumors and conversion in the character of surviving tumor cells from astrocytoma to oligodendroglioma. These data suggest that mTOR activity is required for the survival of some cells within these GBMs, and mTOR appears required for the maintenance of astrocytic character in the surviving cells. Furthermore, our study provides the first example of conversion between two distinct tumor types usually thought of as belonging to specific lineages, and provides evidence for signal transduction–mediated transdifferentiation between glioma subtypes.

Neoplasia (2005) **7,** 356–368

Keywords: Pten, Akt, mTOR, glioblastoma, survival.

Introduction

Glioblastoma multiforme (GBM) is the most frequent and malignant glioma. Disruption of the cell cycle arrest pathway is common and usually achieved by loss of *INK4a-ARF* in these tumors [1]. In addition, overexpression or gain-of-function mutations of receptor tyrosine kinases, such as epidermal growth factor receptor (*EGFR*), platelet-derived growth factor receptor (*PDGFR*), and fibroblast growth factor receptor (*FGFR*) are frequent [2–5], leading to constitutive activation of RAS/MAPK, PI3K/AKT, and other signal transduction pathways. Indeed, the activity of RAS is elevated in the vast majority of GBMs [6], and the activity of AKT is elevated in a majority of the examined GBMs [7,8]. Although no activating mutations in the *AKT* gene are seen in GBMs, AKT is associated with loss of function of PTEN (phosphatase and tensin homology deleted on chromosome 10). Approximately 50% to 70% of GBMs have *PTEN* deletion, mutation, or loss of PTEN expression, implicating *PTEN* as one of the most affected genes in this disease [9–11].

PTEN is mutated or deleted in a large variety of cancers, including GBMs, endometrial cancer, and prostate cancer, and has been well recognized as a tumor suppressor [12–15]. PTEN is a lipid phosphatase as well as a protein phosphatase, and the lipid phosphatase activity is essential for its function as a tumor suppressor [16]. PTEN antagonizes the function of phosphoinositide 3-kinase (PI3K) by dephosphorylating phosphatidylinositol 3,4,5-triphosphate [PtdIns(3,4,5)P_3] at the D3 position [17]. PtdIns(3,4,5)P_3 facilitates the translocation of AKT to the plasma membrane. PtdIns(3,4,5)P_3 also activates PDK1, which then phosphorylates and activates AKT [18–20]. Thus, loss of PTEN function leads to increased AKT activity.

AKT activity promotes cell survival and proliferation through phosphorylation and inactivation of Bad, GSK-3β, FOXO, IKK, and caspase 9 [21]. AKT also activates the mammalian target of rapamycin (mTOR) through TSC1/2 and Rheb [22,23], which in turn phosphorylate p70 S6 kinase (S6K1) and 4E-BP1 [24]—two key regulators for protein synthesis. Phosphorylation of S6 ribosomal protein by S6K1 has been proposed to increase the translation of a group of mRNA containing an oligopyrimidine tract at their 5′ termini (5′ TOP), which encode ribosomal proteins and elongation factors [25]. Phospho-4E-BP1 dissociates from the complex with the translational initiation factor eIF4E, and the free eIF4E can enhance cap-dependent translation [26]. In mouse glia, Akt activity cooperates with

Address all correspondence to: Eric C. Holland, 1275 York Avenue, New York, NY 10021. E-mail: hollande@mskcc.org

[1]This work was supported by NIH grant U01CA894314-1 and by the Seroussi and Bressler Scholars Foundations.

Received 3 September 2004; Revised 3 September 2004; Accepted 18 September 2004.

DOI 10.1593/neo.04595

Ras to specifically recruit existing mRNA encoding growth-promoting proteins to ribosomes [27].

Several studies have suggested a linear oncogenic pathway of PTEN/AKT/mTOR. First, *PTEN*$^{-/-}$ tumors have higher AKT and mTOR activity. Second, the mTOR inhibitor, rapamycin, reduces tumor cell proliferation and tumor growth, but has no effect on *PTEN*$^{+/+}$ tumors, suggesting that mTOR is responsible for the oncogenic effect of PTEN loss [28,29]. In addition, mTOR is required for cell transformation by PI3K and AKT [30]. Moreover, in human GBMs, mTOR activity correlates with AKT activity [31,27], raising the possibility that the oncogenic effect of AKT might be achieved through mTOR.

We previously reported that the somatic cell gene transfer by the RCAS/*tv-a* modeling system of constitutively activated *Akt* and *KRas* cooperatively induces GBMs from neural progenitors, but not from differentiated astrocytes [8]. In addition to its oncogenic effect, Akt activation in glial tumors also leads to astrocytic differentiation [32,33]. In human GBMs, *PTEN* mutation or deletion is very common, but no activating mutations of *AKT* have been found. It remains to be determined whether PTEN loss alone is sufficient to achieve the oncogenic effect of activated AKT in GBM formation. Besides AKT, loss of PTEN function activates other factors such as SHC and FAK [34–36]. Whether activated AKT fully recapitulates the oncogenic function of PTEN loss is unknown. If PTEN loss is equivalent to activated AKT in tumorigenesis, therapeutic targeting of molecules downstream of AKT in *PTEN*-null GBMs would be justified; if PTEN loss is insufficient to achieve the oncogenic effect of AKT, *anti-receptor* tyrosine kinase therapy might be necessary for those tumors. Because homozygous *Pten* deletion in mice results in embryonic lethality, we addressed this question by conditional targeting of *Pten* in glia with the combination of RCAS/*tv-a* and Cre/Lox systems.

mTOR has been proposed to be an important factor in the signaling downstream of AKT; we therefore investigated whether its activity is elevated and required for the maintenance of *Akt*+*KRas*–induced GBMs by blocking mTOR with a rapamycin analog, CCI-779. The CCI-779 treatment of mouse GBMs results in two effects. A subset of tumor cells with elevated Akt undergo apoptosis on mTOR blockade, indicating that mTOR activity is required for survival of those tumor cells. Furthermore, the surviving tumor cells convert their astrocytic character to oligodendroglial morphology, suggesting that mTOR is also required to maintain astrocytic character in these GBMs.

Results

Generation of Conditional Glia-Specific Pten Mutant Mice

Mouse mutants in which *Pten* exons 4 and 5 are flanked by *LoxP* sites have been described before [37]. *tv-a* mice expressing tv-a in neural progenitors (*Ntv-a*) [38] or predominantly in astrocytes (*Gtv-a*) [39] were crossed with the *Pten*$^{loxP/loxP}$ (*LP*) mice, and the homozygous *tv-a* *Pten*$^{loxP/loxP}$ (*Ntv-a LP*; *Gtv-a LP*) mice were obtained. The Cre recombinase fused with the green fluorescent protein (GFP) encoded by the RCAS vector allows recombination between the *LoxP* sites in progenitors or astrocytes, leading to *Pten* deletion in those cells.

To test whether this strategy works, primary brain cells from *Ntv-a LP* mice were infected with RCAS-*Cre* or control RCAS-*LacZ* virus. Due to the heterogeneity of the cell population and infection efficiency, only some of the neural progenitors were infected by the RCAS virus. Subsequently, polymerase chain reaction (PCR) analysis showed that Cre specifically catalyzed recombination and *Pten* deletion in the infected progenitors, whereas the *Pten* gene in other types of cells and the uninfected neural progenitors remained intact (Figure 1*B*).

Loss of Pten in Cultured Neural Progenitors Activates Akt, But Does Not Activate MAPK Pathway

We next studied the consequence of Pten loss in glial cell culture. We observed that Cre decreased Pten protein level and activated Akt to a similar level as that of RCAS-*Akt*–infected primary brain cells cultured in medium with 10% fetal bovine serum (FBS) from *Ntv-a LP* mice (data not shown). To avoid PI3K/Akt activation by growth factors in the serum, primary brain cells from *Ntv-a LP* mice infected with the RCAS viruses were cultured in serum-free medium for 24 hours. Western blot analysis showed that Cre led to a significant reduction in Pten levels and the consequent increase in phospho-Akt (P-Akt) similar to cells infected with the RCAS-*Akt* virus that encodes a constitutively active Akt. This observation implies that loss of Pten alone is sufficient to achieve a high level of activated Akt in cultured progenitors. Cre itself did not change Pten expression or Akt activity in primary brain cells from *Ntv-a* wild-type (*wt*) mice. Total Akt protein levels decreased in cells infected with RCAS-*Akt*, RCAS-*Cre*, RCAS-*Akt*+RCAS-*KRas*, and RCAS-*Cre*+RCAS-*KRas*, suggesting that elevated Akt activity in those cells exerted a negative feedback on Akt protein levels. This is consistent with a previous finding stating that, in human GBMs, elevated AKT activity correlates with decreased total AKT protein levels [8]. Cre-induced *Pten* deletion did not result in activation of Erk, suggesting that loss of Pten did not activate the MAPK pathway in progenitors. Elevated Ras activity achieved by RCAS-*KRas* infection did not activate PI3K/Akt pathway as measured by P-Akt levels. However, KRas, in combination with Akt or Cre, led to activation of both MAPK and PI3K/Akt pathways (Figure 1*C*).

Loss of Pten Cooperates with KRas Activation to Induce GBMs from Neural Progenitors

Our previous work demonstrated that the combination of *KRas* and *Akt* induces GBMs from neural progenitors with an incidence of 21.3% [8,32]. To investigate the function of Pten loss in tumorigenesis, 37 newborn *Ntv-a LP* mice were injected intracranially with a combination of cells producing RCAS-*KRas* and RCAS-*Cre*. All the mice were sacrificed at 12 weeks of age, or earlier if they showed signs or symptoms of macrocephaly and lethargy. The mouse brains were

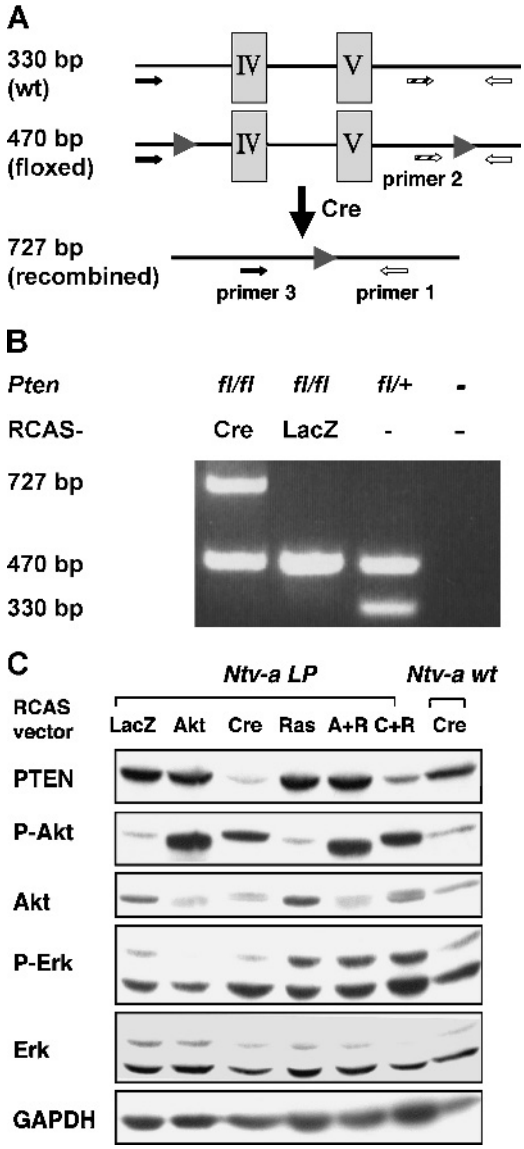

Figure 1. *Combined RCAS/tv-a and Cre/Lox systems result in Pten deletion and consequent Akt, but not MAPK pathway activation. (A) Schematic representation of the location of PCR primers to detect the wild-type (wt), floxed, and recombined Pten allele. (B) PCR analysis indicates that RCAS-Cre resulted in Pten deletion in some of the neural progenitors (lane 1, upper band) from Ntv-a LP mice, but not in other types of primary brain cells or uninfected neural progenitors (lane 1, lower band). DNA of RCAS-LacZ–infected primary Ntv-a LP brain cells (lane 2), tail DNA from Ntv-a LP$^{+/-}$ (lane 3), and dH_2O (lane 4) were used as controls. (C) Western blot analysis shows that Cre decreased Pten protein level and consequently activated the Akt pathway, but not the MAPK pathway, in neuronal progenitors from Ntv-a LP mice. GAPDH was used as a loading control.*

Supplementary Figure 1. *Low-power views (100×) of GFAP/Olig2 staining in the untreated and 7-day–treated mouse GBMs. In contrast to the IHC of GFAP in the untreated tumors (A), the pattern of GFAP staining in the 7-day–treated tumors was similar to that in oligodendrogliomas, and GFAP-positive cells were reactive astrocytes. In the untreated tumors, Olig2 staining was very heterogeneous. There was no Olig2-positive cells in approximately 90% of microscopic views (B), and (C) represents a view with maximum Olig2-positive cells. (E) and (F) show that almost all surviving tumor cells in two treated tumors were Olig2-positive, and that Olig-2 negative cells were reactive with astrocytes and vascular cells. The asterisks in (F) indicate areas of necrosis.*

fixed and the sections were stained with hematoxylin and eosin (H&E).

Of the 37 *Ntv-a LP* mice, 23 (62.2%) developed parenchymal lesions that varied in size. Histologically, these lesions showed increased cell density, pseudopalisading necrosis, microvascular proliferation, and nuclear pleiomorphism that looked similar to *KRas+Akt*–induced GBMs in *Ntv-a wt* mice (Figure 2*A*). Immunohistochemical staining (IHC) analysis demonstrated that Pten was absent in the tumor cells but present in the surrounding normal brain cells and endothelial cells within the tumors (higher magnification not shown). The tumor cells stained positive for phospho-Erk, indicating that they were infected by RCAS-*KRas*. They were proliferating, as shown by positive staining for proliferating cell nuclear antigen (PCNA), and they also expressed nestin and glial fibrillary acid protein, indicating their glial origin (Figure 2*B*). Some of the tumors are strongly positive for GFAP (Figure 2*C*)—one characteristic of human GBMs.

A finding consistently associated with both *KRas+Akt* and *KRas+Pten* loss tumors of all sizes was a conspicuous inflammatory element including perivascular infiltration by small lymphocytes and parenchymal histocytic infiltrates that virtually obscured the neoplastic component of some early evolving lesions. GFAP and nestin expression on the part of atypical cells revealed neoplastic populations in some small lesions accompanied by florid lymphohistocytic responses. To what extent this observation in mice represents the characteristics of early high-grade human gliomas is not known.

We determined whether loss of Pten alone is sufficient to cause GBMs by infecting 32 *Ntv-a LP* mice with RCAS-*Cre* and found that no tumors arose. This result is similar to our earlier studies that *Akt* alone is insufficient to induce GBMs [8]. RCAS-mediated gene transfer of *KRas* and *Cre* did not result in GBM formation in *Gtv-a LP* mice ($n = 23$), consistent with the observation that the combination of *KRas* and *Akt* is unable to induce GBMs in *Gtv-a wt* mice [8]. Cre has been shown to cause chromosomal aberrations, which may potentially increase tumor susceptibility [40]. We thus infected 19 *Ntv-a wt* mice with RCAS-*KRas* and RCAS-*Cre* to test the specificity of the recombination at the *Pten* locus. None of these mice developed tumors, suggesting that it is the Cre-induced *Pten* deletion that contributes to tumor formation (Figure 3*A*). However, the genetic backgrounds of *Ntv-a wt* and *Ntv-a LP* mice were different, which could affect the size or number of tumors induced by *KRas* and *Akt*.

Therefore, to compare the function of Pten loss and activated Akt in the same genetic background, 37 newborn *Ntv-a LP* mice were infected with RCAS-*KRas* and RCAS-*Akt*. Eighteen mice (48.6%) developed GBMs, which were histologically indistinguishable from *KRas+Pten*–null tumors (Figure 3*B*). The tumor incidences of these two groups of mice were not statistically different ($P = .61$).

We previously generated GBMs with the combination *KRas* and *Akt* in *Ntv-a wt* mice [8,32], and there was a certain percentage of large-sized and medium-sized tumors. In contrast, we observed that most tumors induced in *Ntv-a LP* mice by *KRas* and *Pten*-null or *KRas* and *Akt* were small, and the distribution pattern of these GBMs differs from *KRas+Akt*–induced GBMs in *Ntv-a wt* mice (Figure 3, *C* and *D*). In addition, the tumor incidences of *Ntv-a LP* mice were statistically higher than that of *Ntv-a wt* mice ($P < .01$; Figure 3*D*). Therefore, it appears that the genetic background

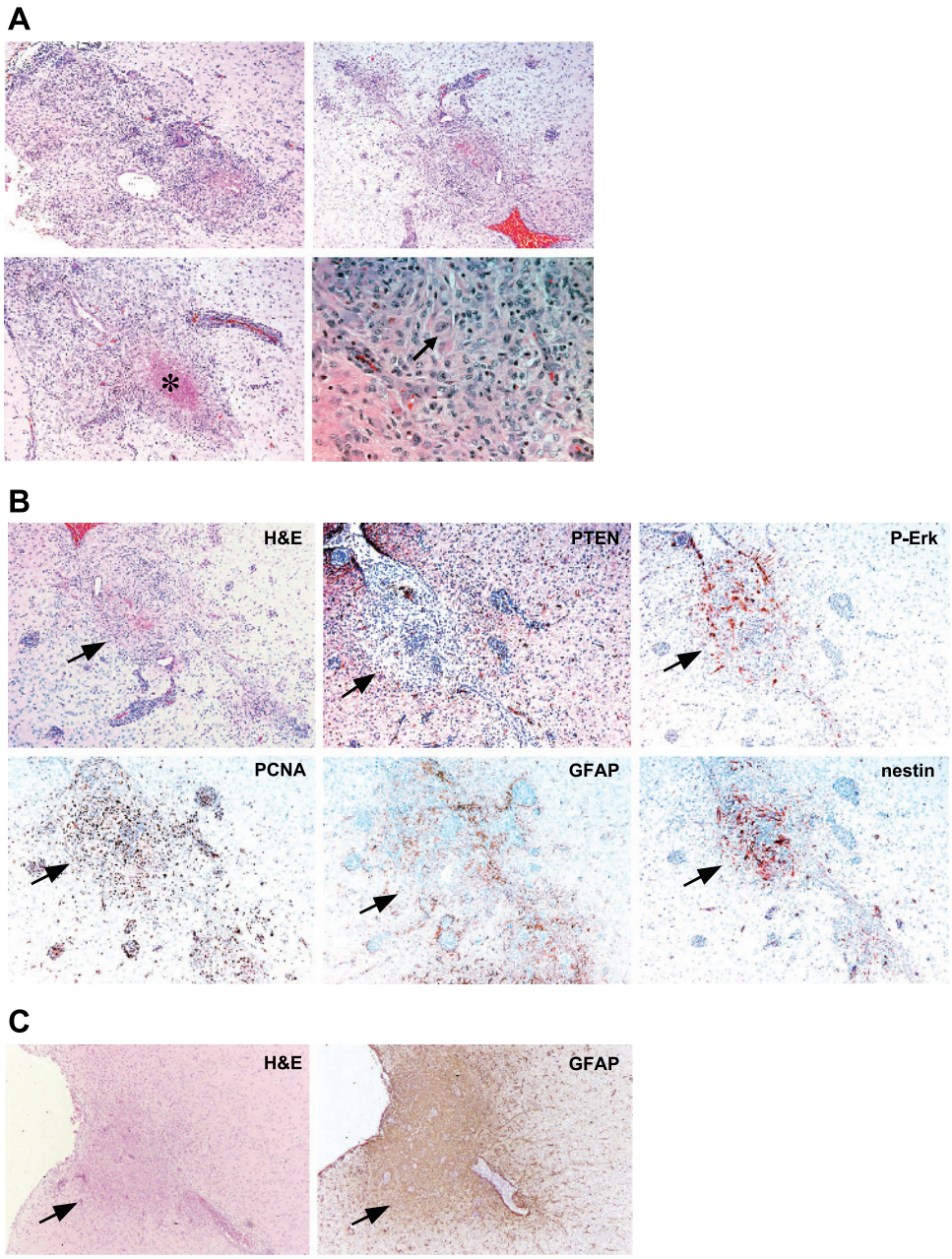

Figure 2. *Histologic analysis of GBMs induced by Cre+KRas from Ntv-a LP mice (A) H&E–stained sections illustrates increased cell density, pseudopalisading necrosis (asterisk), microvascular proliferation, and nuclear polymorphism (arrow) (original magnification of pictures on the upper panel and lower left panel, 40×; original magnification of the picture on the lower right panel, 400×). (B) (40×) IHC shows that Pten was absent in the tumor cells but present in the normal brain cells and endothelial cells within the tumors (higher magnification not shown). The tumor cells were positive for P-Erk and PCNA, and some of them were positive for GFAP and nestin. (C) (50×) IHC shows that some GBMs stained strongly positive for GFAP—one of the characteristics of human GBMs.*

of *Ntv-a LP* mice made them more susceptible to tumor initiation but less to tumor progression.

Activated Akt alone is unable to induce GBMs in *Ntv-a Ink4a-Arf*$^{-/-}$ mice [32]. To further investigate the similarities of Pten loss and Akt activation, we determined whether loss of Ink4a-Arf and Pten cooperates to form GBM. We infected 27 *Ntv-a Ink4a-Arf*$^{-/-}$ *LP* mice with RCAS-*Cre* and found that no tumors developed, indicating that loss of combined *Ink4a-Arf* and *Pten* is insufficient for tumor formation. In summary, the above data suggest that Pten loss and activated Akt function similarly in tumorigenesis.

mTOR Activity Correlates with Activated Akt in Akt+KRas–Induced GBMs

mTOR has been proposed to be an important component downstream of the Akt signaling pathway. We therefore initially tested whether the phospho levels of S6 downstream of mTOR correlate with Akt activity in the *KRas+Akt–*induced tumors from *Ntv-a wt* mice. As the RCAS-encoded constitutively active Akt construct contains an *HA* tag sequence, detection of HA represents the retroviral expression of the activated Akt. The tumors were immunostained with an anti-HA antibody, and the adjacent sections were

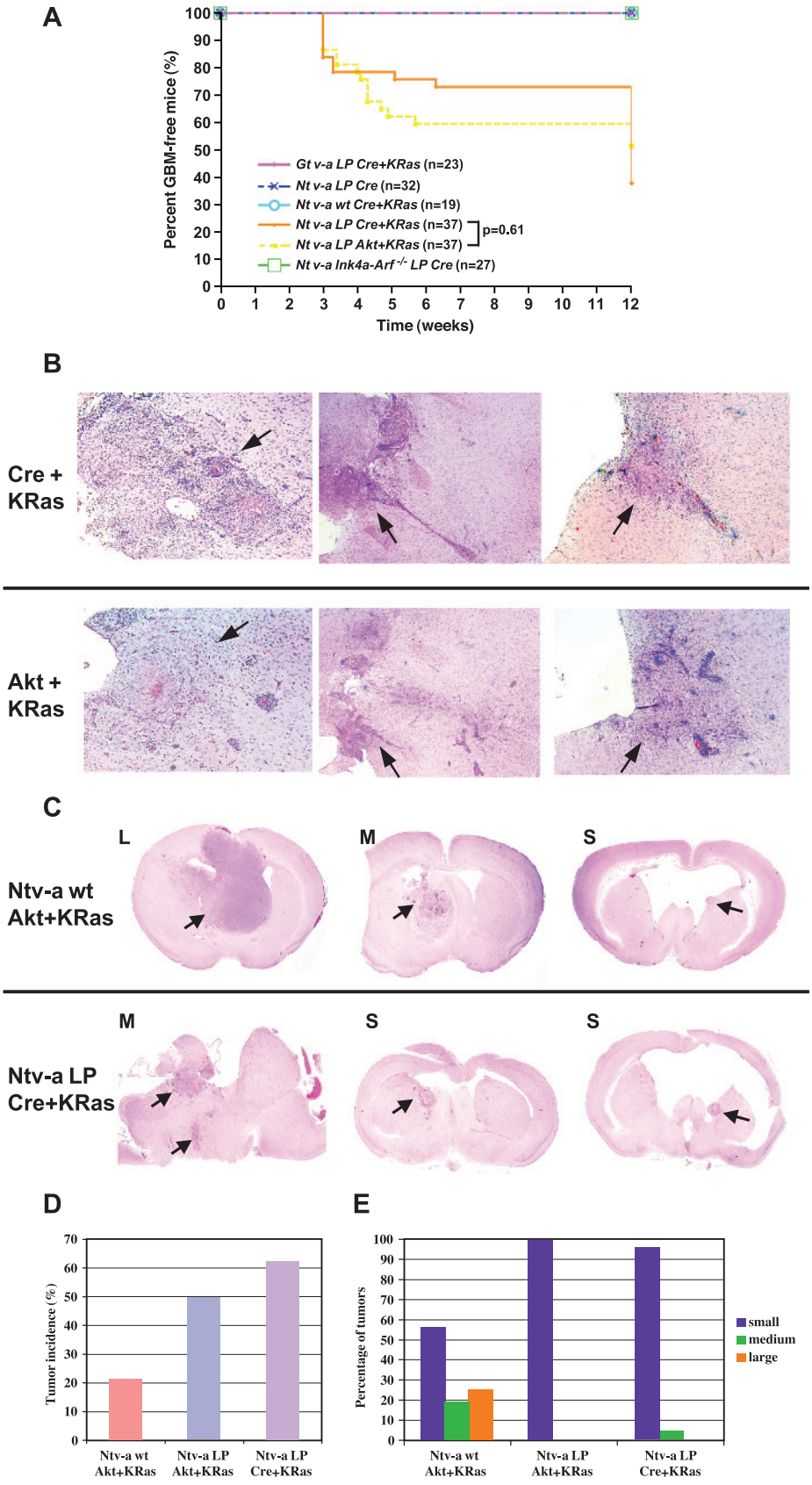

Figure 3. *Loss of Pten is similar to activated Akt in gliomagenesis. (A) Percent GBM-free mice curves indicate that Cre+KRas and Akt+KRas induced GBMs from Ntv-a LP (nestin-expressing neuronal progenitors) with no significant difference in tumor incidence (62.2% vs 48.6%; P = .61). (B) (10×) H&E comparison of the GBMs induced by Cre+KRas and Akt+KRas from Ntv-a LP mice shows similar tumor morphology. (C) (10×) In Ntv-a wt background, Akt+KRas resulted in large (L), medium (M), and small (S) GBMs; whereas in Ntv-a LP background, Cre+KRas led to only one medium-sized GBM and most GBMs were small. (D) Tumor incidence was higher in Ntv-a LP mice compared to Ntv-a wt mice (P < .01). (E) Percentage of large-sized and medium-sized tumors was higher in Ntv-a wt mice.*

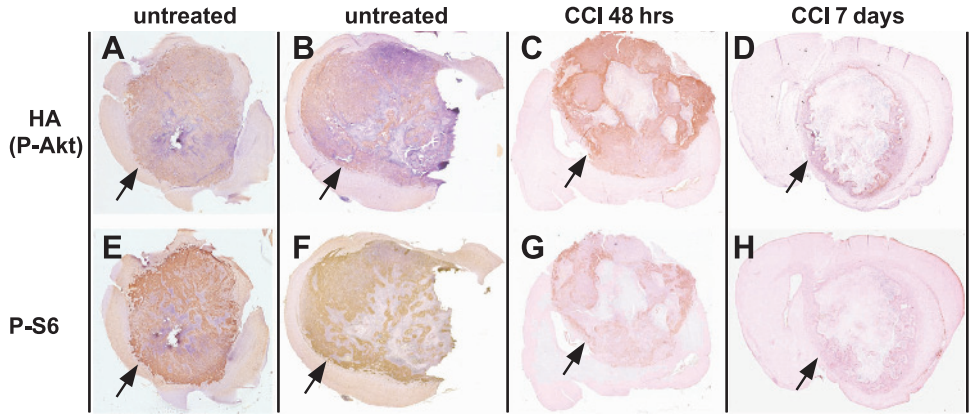

Figure 4. *mTOR activity correlates with activated Akt in Akt+KRas–induced GBMs, and mTOR blockade by CCI-779 decreases P-S6 in the surviving tumor cells. (10×) IHC for HA (representing P-Akt) (A and B) and P-S6 (E and F) on adjacent sections from Akt+KRas–induced GBMs suggests that mTOR activity as measured by P-S6 correlates with activated Akt. (C and G) (10×) IHC of HA and P-S6 on adjacent sections from the Akt+KRas–induced GBM treated with CCI-779 for 48 hours. (D and H) (10×) IHC of HA and P-S6 on adjacent sections from the Akt+KRas–induced GBMs treated with CCI-779 for 7 days.*

immunostained with an antibody against phospho-S6 (P-S6). Within these tumors, there was regional variation in HA staining, implying that Akt activity was also regionally variable. The tumor cells positive for HA were also positive for P-S6 (Figure 4, *A*, *B*, *E*, and *F*), suggesting that mTOR pathway is upregulated and that it correlates with activated Akt in this mouse GBM model.

Treatment of GBM-Bearing Mice with an mTOR Inhibitor, CCI-779

We then investigated whether mTOR activity is required for tumor maintenance *in vivo*. First, we generated GBMs from *Ntv-a wt* mice with the combination of RCAS-*KRas* and RCAS-*Akt*. Mice showing signs of macrocephaly or lethargy were then screened for GBMs with magnetic resonance imaging (MRI), which has been previously described [41]. Large tumors were detected by enhancement with intravenous contrast, indicating disruption of the blood–brain barrier. These tumors exhibited histologic characteristics of human GBMs including pseudopalisading necrosis, pleiomorphism, and microvascular proliferation. These mice were chosen because their response to mTOR blockade would better reflect the therapeutic effects of mTOR inhibitors on human GBMs. Five mice with GBMs were treated with CCI-779, a rapamycin analog, through intraperitoneal injection. Although 0.1 mg/kg per day is the biologic active dose for xenograft tumors [28], the dose of CCI-779 required to affect its target in the mouse brain varies and is much higher. The biologic active doses in the cerebellum and hippocampus are 25 and 10 mg/kg per day, respectively [28,42]. We therefore chose a daily dose of 40 mg/kg to ensure the inhibition of mTOR activity in mouse GBMs. Because of the large size of these tumors at the onset of treatment, the mice survived for 2 to 7 days and the brains were analyzed.

Two of these mice survived for 7 days and could be reimaged. The MRI results showed that the original contrast enhancement was reduced, suggesting that the tumor biology was affected by CCI-779 (Figure 5*A*). The histologic analysis of these tumors showed two effects: regional tumor cell death and morphologic conversion of surviving tumor cells.

mTOR Blockade Leads to a Subset of Tumor Cells Undergoing Apoptosis

One mouse became morbid after 48-hour treatment and was sacrificed. Within this tumor, there were sheets of dead tumor cells with picnotic nuclei, in contrast to psudopalisading necrosis in the untreated tumor (Figure 5*B*). Seven-day treatment in the other four mice resulted in a similar regional tumor cell death or dramatic killing of tumor cells.

To assess the effect of CCI-779 on these tumors, adjacent brain sections were immunostained with HA and P-S6 antibodies. In the untreated GBMs, most tumor cells express variable amounts of activated Akt (HA positive), and P-S6 levels correlates with activated Akt (Figure 4, *A*, *B*, *E*, and *F*). The reason for this observed variability in untreated GBMs is unknown, but may partly be due to the oligoclonal nature of gliomas generated by RACS vector infection. However, the brain analyzed after a 48-hour treatment showed more extensive cell death surrounded by surviving HA-positive tumor cells; immunostaining for P-S6 was markedly reduced in the majority of HA-positive tumor cells. In the brain treated for only 48 hours, some surviving HA-positive tumor cells were also positive for P-S6, possibly because the drug had not effectively inhibited mTOR activity in these regions (Figure 4, *C* and *G*). In contrast, 7-day treatment led to nearly complete loss of P-S6 in the surviving tumor cells that were positive for HA (Figure 4, *D* and *H*). The lack of correlation between HA and P-S6 staining in these tumors treated for 7 days is consistent with blockade of mTOR activity.

Given the appearance of cell death on mTOR blockade in the GBMs, we performed "TdT - mediated dUTP nick end labeling (TUNEL) assays to determine whether those cells underwent apoptosis. Indeed, the areas of cell death were strongly positive for TUNEL, implying apoptosis occurring in a subset of the tumor cells within as early as 48 hours

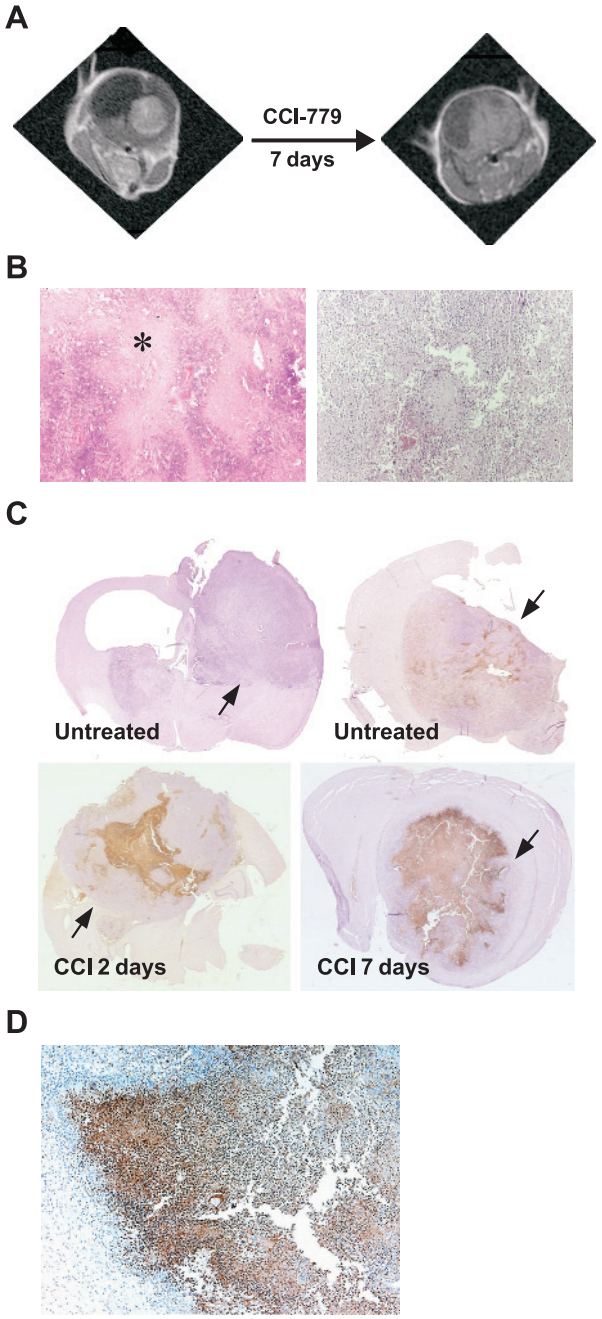

Figure 5. *mTOR blockade induces apoptotic death in GBM cells expressing activated Akt. (A) MRI with contrast enhancement images shows loss of enhancement in a mice bearing GBM after 7-day CCI-779 treatment. (B) (40×) H&E–stained sections demonstrate that in contrast to psudopalisading necrosis in the untreated GBMs (left panel), 48-hour CCI-779 treatment resulted in apoptotic cell death in the tumor (right panel). The asterisk indicates one representative area of pseudopalisading necrosis. (C) (10×) TUNEL assay shows that CCI-779 treatment led to regional apoptotic cell death (brown color). (D) (400×) Higher magnification of the TUNEL assay results from a mouse GBM treated with CCI-779 for 7 days.*

(Figure 5*C*, *lower panel*; Figure 5*D*). In contrast, there were few endogenous apoptotic cells in the untreated GBMs, and these cells were mostly near necrotic areas (Figure 5*C*, *upper panel*). These results provide evidence that mTOR blockade resulted in regional apoptosis in the tumor cells. As the surviving tumor cells after 7-day mTOR blockade express a relatively lower amount of HA (Figure 4*D*), it is possible that CCI-779 treatment resulted in regional killing of GBM cells expressing high levels of Akt activity, and that GBM cells with low levels of Akt activity survived mTOR inhibition.

mTOR Blockade Results in Conversion of Surviving GBM Cells to an Oligodendroglioma-Like Morphology

Astrocytomas are thought to arise from astrocytes or their precursors, and express an astrocytic marker, GFAP [43]. GBMs are the most malignant subtype of astrocytoma and maintain the astrocytic character. *KRas+Akt*–induced GBMs exhibit typical characteristics of human GBMs [8]. These untreated mouse tumor cells have heterogeneously elongated nuclei and fibrillary cytology. However, in three of four GBMs that were treated with CCI-779 for 7 days, we observed that the vast majority of surviving tumor cells was of a different morphology. Some regions of the surviving tumor cells in one GBM treated for 7 days also showed a similarly changed morphology. All those tumor cells consisted of homogenous, round nuclei surrounded by cleared cytoplasm (Figure 6*A*, *lower left panel*). In addition, the tumors showed perineuronal satellitosis and perivascular satellitosis in areas of cortical invasion (data not shown). These features resemble the histologic characteristics of *PDGF*-induced murine oligodendrogliomas [44], which have been shown to contain low Akt activity. To evaluate the shifted tumor morphology at molecular level, we performed immunohistochemistry using an antibody for Olig2, a lineage marker for neural progenitors and oligodendrocytes that is uniformly expressed in a high percentage of oligodendroglioma cells [45,46]. Seventy-five to 85% of the surviving cells in the three GBMs that exhibited massive morphologic change were strongly positive for Olig2. In contrast, analysis of untreated GBMs revealed that less than 10% of cells in the tumors were Olig2-positive and that their distribution was very heterogeneous (Figure 6, *A* and *C*; Supplementary Figure 1). Although one 7-day–treated GBM exhibited only partially changed glioma morphology and approximately, 23% of the surviving cells were Olig2-positive; typical oligodendroglioma morphology was exclusively seen in the GBMs treated for 7 days but not in the untreated ones. Overall, the percentage of Olig2-positive cells in the 7-day–treated GBMs was statistically significant compared to that of the untreated GBMs ($P < .01$). The surviving tumor cells were negative for other oligodendroglial markers, including A2B5, O4, MBP, and PLP (data not shown), with the exception that a small percentage of treated tumor cells were positive for CNPase. This result is consistent with the fact that none of these markers stains human oligodendrogliomas either [47]. Similar to oligodendrogliomas, the tumor cells with shifted morphology in the treated GBMs were immunonegative for GFAP, except for the scattered entrapped reactive astrocytes (Figure 6*A*). Taken together, both morphologic and immunohistochemical similarities indicate that the surviving GBM cells are converted to oligodendroglioma cells. However, the GBM treated with CCI-779 for only 48 hours showed astrocytic morphology and low Olig2 staining consistent with the above-mentioned residual S6 activity in these cells (data not shown). It is

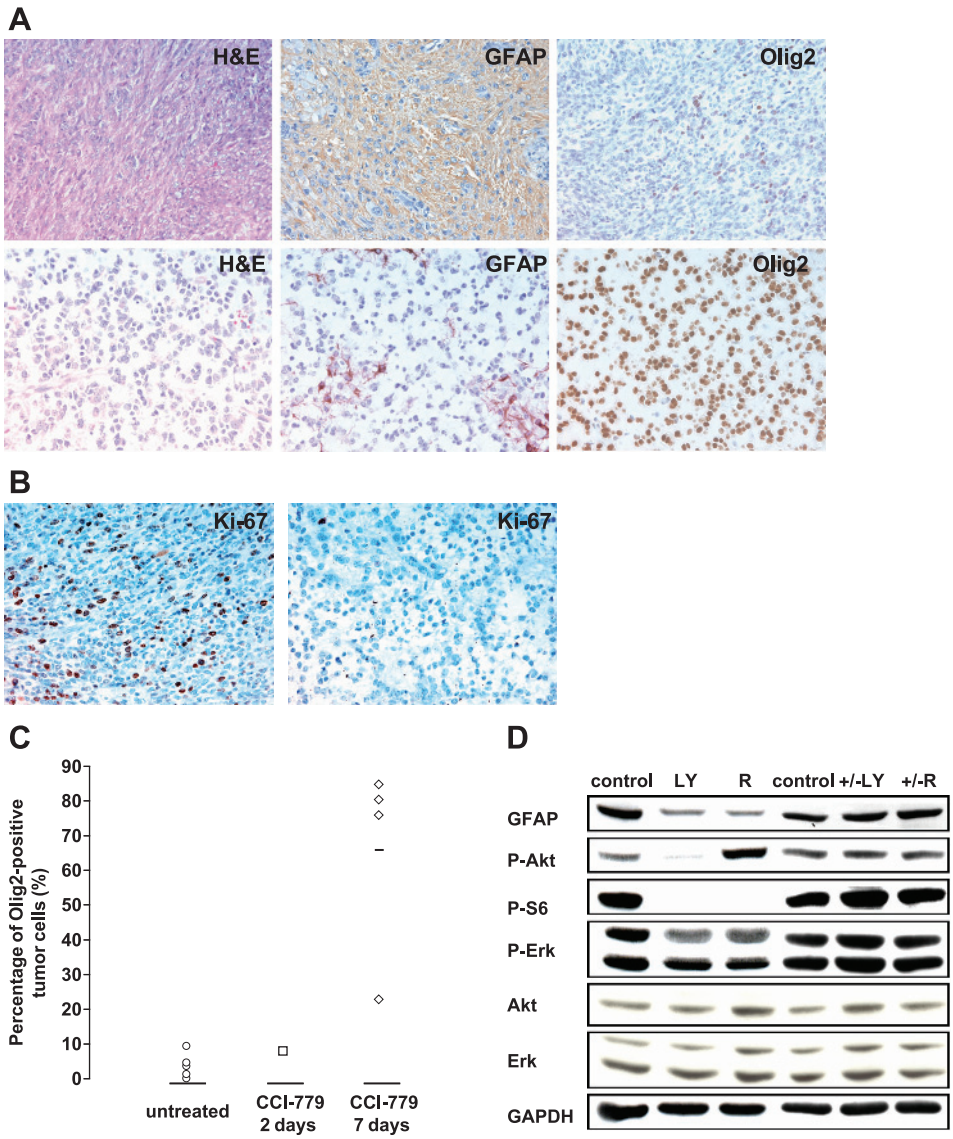

Figure 6. *mTOR blockade converts surviving tumor cells to an oligodendroglioma-like morphology (A) (400×) Histology comparison of untreated (upper panel) and 7-day–treated GBMs (lower panel) induced by Akt+KRas. Untreated GBM cells showed fibrillary cytology; they were positive for GFAP but most of them were negative for Olig2, as indicated by H&E and IHC. In contrast, surviving tumor cells acquired oligodendroglioma morphology with round nuclei and cleared cytoplasm; GFAP-positive cells were reactive astrocytes; and most of the tumor cells were positive for Olig2. (B) (400×) IHC of Ki-67 in the untreated (left panel) and 7-day–treated GBMs shows that mTOR blockade inhibited proliferation of the surviving tumor cells. (C) Percentage of Olig2-positive cells in 7-day–treated GBMs was much higher than that in the untreated tumors ($P < .01$). Each symbol represents one tumor, and "–" represents the mean value for each tumor group. (D) mTOR inhibition decreases GFAP protein level in primary astrocytes. Selected primary astrocytes from Gtv-a wt mice were treated with 10 BM LY294002 (LY) or 10 nM rapamycin (R) for 6 days. After 6 days, cells treated with inhibitors were cultured in medium without inhibitors for an additional 6 days (+/–LY, +/–R). The control cells were mocked-treated for 6 days (lane 1) or 12 days (lane 4). Western blot analysis shows that LY294002 inhibited P-Akt and P-S6, and that rapamycin inhibited P-S6, but the inhibitors did not affect P-Erk significantly. LY294002 and rapamycin inhibited GFAP protein to a similar level, whereas astrocytes began to express GFAP after removal of the inhibitors.*

possible that 48 hours is insufficient to achieve complete mTOR blockade and morphologic conversion in the surviving tumor cells.

There are two potential explanations for the conversion of morphology for the tumor cell population. First, the low percentage of Olig2-positive cells may not have been affected by CCI-779, and thus their population expanded during the week of treatment. Second, it is also possible that the surviving tumor cells were dependent on mTOR for maintaining astrocytic character. Thus, rather than undergoing apoptosis, they changed their morphology on mTOR inhibition. To distinguish between these two possibilities, we performed immunohistochemistry with a proliferation marker Ki-67 antibody to determine if the cells with oligodendrocytic morphology were proliferating and capable of giving rise to the residual tumor mass. We found that in contrast to the untreated GBM cells, proliferation was significantly inhibited in surviving cells of GBMs treated with CCI-779 (Figure 6*B*), suggesting that surviving tumor cells acutely converted their morphology and that mTOR is required to maintain their astrocytic character.

Akt activity shifts *KRas*-induced nonastrocytic sarcomas in an *Ink4a-Arf*–deficient background to an astrocytic GBM

morphology [32]. Previous data from our laboratory have shown that activity of the Akt pathway is not elevated in *PDGF*-induced oligodendrogliomas and that addition of activated Akt converts *PDGF*-induced oligodendrogliomas to astrocytomas. These data imply that elevated Akt activity plays an important role in astrocytic differentiation of glioma cells. Moreover, the above results from mTOR inhibition in the astrocytic GBMs suggest that Akt signaling in astrocytic differentiation is achieved through mTOR. We therefore further tested this hypothesis with an *in vitro* cell culture experiment. Primary brain cells were prepared from *Gtv-a wt* mice and infected with RCAS-*puro* virus. Astrocytes were selected with puromycin and then treated with 10 μM LY294002, a PI3K inhibitor, or 10 nM rapamycin for 6 days. We observed a decrease in cellular processes on treatment (data not shown). PI3K inhibition with LY294002 and mTOR inhibition with rapamycin decreased GFAP protein to similar levels, suggesting that the GFAP inhibition by LY294002 is mainly through mTOR blockade (Figure 6*C*, *left three lanes*). The inhibition was not due to cell death because after the inhibitors were removed and cells were allowed to recover for an additional 6 days, they began to reexpress GFAP (Figure 6*C*, *right three lanes*). These results further support the idea that mTOR is required to maintain the astrocytic character of glial cells.

To determine if the effect we were seeing could have parallels in cultured primary brain cells, we measured protein levels of other oligodendrocytic markers including Olig2, A2B5, O4, CNPase, MBP, and PLP as a function of mTOR blockade by Western blot analysis. None of these markers was detectable in the control-treated or inhibitor-treated primary astrocyte cultures. The data imply that mTOR activity may not regulate the conversion of one glial lineage to another even though it does regulate the conversion of glioma subtypes. Therefore, these glioma subtypes may not simply be transformed versions of oligodendrocytes and astrocytes.

Discussion

GBM is a genetically complex disease. Upstream growth factor receptor activation and loss of PTEN function both lead to activation of the AKT signaling pathway, which has been shown to be causal in gliomagenesis. In human GBMs, disregulation in *PTEN*, but not *AKT*, is seen. The early embryonic lethality of *Pten*$^{-/-}$ mice has precluded further studies of the role of Pten loss in GBM formation [13–15]. Here, we recapitulate the genetic aberration seen in human GBMs and demonstrate that loss of Pten function is similar to hyperactivated Akt in gliomagenesis. Consistent with our previous study of Akt in tumorigenesis, Pten loss alone is insufficient to cause GBMs from neural progenitors, or from progenitors deficient for *Ink4a-Arf*. KRas combined with loss of Pten function leads to GBM formation from neural progenitors, but not from differentiated astrocytes. The tumor incidence and morphology of the *KRas+Pten* loss–induced GBMs are similar to *KRas+Akt*–induced GBMs. These results demonstrate the relationship between Pten loss and Akt in two ways. First, it suggests that much of the oncogenic effect of Pten loss appears to be due to Akt activity. Second, it indicates that, at least in culture, Pten loss alone is sufficient to elevate Akt to oncogenic levels without activation of upstream growth factor signaling. The mouse studies imply that AKT and its downstream effectors could be critical therapeutic targets for treatment of *PTEN*$^{-/-}$ GBMs. Although *PTEN* mutation or deletion is a frequent genetic event found in human GBMs, our studies suggest that disregulation of the gene alone appears to be insufficient to cause GBM formation. This observation is supported by data from other research groups, which showed that inactivation of Pten in neural progenitors or granule neurons of the dentate gyrus and cerebellum could not elicit neoplastic transformation in the brain [48–50]. Moreover, in our study, neural progenitors deficient for both *Pten* and *Ink4a-Arf* do not give rise to GBMs, suggesting that additional genetic alterations are required for tumor formation in this context.

Many studies have been focused on PTEN as an antagonist of PI3K/AKT signaling pathway. Although PTEN may have other functions, such as downregulation of MAPK pathway through dephosphorylation of SHC [35,36], our *in vitro* experiment suggests that this is not occurring in glial cells. Pten has also been shown to inhibit tumor invasion independent of its lipid phosphatase activity [51], or possibly through dephosphorylation of FAK [34]. In addition, Pten can regulate p53 protein levels and activity through phosphatase-independent mechanisms [52]. In fact, some GBMs harbor *PTEN* mutations outside the sequences encoding the phosphatase domain, which may not affect its phosphatase activity [53]. Our data suggest that although these functions may be occurring, they appear not to be required for gliomagenesis.

There is emerging evidence suggesting that mTOR is a critical downstream component in PTEN/AKT signaling positively regulating cell growth and survival [54,55]. mTOR has also been implicated as an indirect homeostatic sensor for nutrients and ATP [56]. We demonstrate here that mTOR activity correlates with activated Akt in the mouse GBMs. Within these tumors, the cells expressed virally encoded Akt heterogeneously, potentially due to the oligoclonal nature of RCAS-induced tumors. The tumor cells with elevated Akt appear to be dependent on mTOR for survival, and mTOR blockade in these cells leads to apoptotic cell death. This cytotoxic effect is also seen in a recent study showing that mTOR inhibition in Akt-dependent murine prostate intraepithelial neoplasia induces apoptosis and complete reversion of the neoplastic phenotype [57]. In our experiments, mTOR inhibition did not result in killing of all tumor cells; those with lower active Akt expression survived and changed morphology associated with loss of mTOR activity as measured by phosphorylation of S6.

mTOR inhibitors, including CCI-779, rapamycin, and RAD001, have been disappointing as single agents in clinical trials for GBM patients. Several explanations might account for the different responses in mouse and human studies. First, these patients have not been stratified by AKT activity prior to enrolling them into these trials. Second, the daily

treatment regimen in mice may be more effective in blocking mTOR activity relative to weekly CCI-779 administration in patients. Third, a few GBM patients have, in fact, shown response to rapamycin treatment; our mouse model may reflect the biologic status of this subset of tumors. Finally, human GBM often harbors multiple genetic alterations; it is possible that in the presence of other genetic alterations (not present in the mouse tumors), mTOR is not required for tumor maintenance. Using our genetically simplified Ras+Akt mouse GBM model, mTOR inhibition does not result in complete tumor remission. Studies from Akt-driven lymphomas demonstrated that although mTOR blockade only leads to partial response, it greatly enhances the sensitivity of tumor cells to chemotherapy [58]. Therefore, our mouse data, together with those of others, suggest that inhibition of multiple signaling pathways, in combination with chemotherapy, might be necessary for therapeutic success in human GBM management.

Our previous studies showed that Akt causes astrocytic differentiation in glioma cells [32]. In the *Akt+KRas*–induced GBMs treated with CCI-779, surviving cells acquired an oligodendroglioma-like morphology. We demonstrate that CCI-779 inhibits proliferation of these cells and the conversion from astrocytic to oligodendrocytic character. The surviving cells had lower Akt activity, suggesting that although they are not dependent on mTOR for maintenance, they do require mTOR to maintain astrocytic differentiation.

Several studies have proposed the existence of cancer stem cells in certain central nervous system (CNS) tumors, including gliomas [59–61]. These tumors have been proposed to derive from stem cells or glial-restricted progenitors with accumulation of mutations, and are capable of self-renewing, proliferating, and giving rise to cells of multiple lineages. Previous mouse studies from our laboratory have demonstrated that both activation of signaling pathways and the cell of origin are important for glioma formation and histologic character. In this system, gliomas can arise in mice from either neural progenitors or astrocytes [8,32,44], although nestin-expressing progenitors are far more sensitive to the oncogenic effects of Ras and Akt signaling. The morphology of these gliomas can also be changed by the activity of signaling pathways [32]. Here we demonstrate a transition between the two glioma subtypes induced by mTOR inhibition. This effect appears to not result from expansion of a clonal cell population, but rather from conversion of tumor cell morphology. This observed shift from one apparent glial lineage to another further provides evidence to support an alternative possibility that the existence of tumors apparently containing multiple lineages may reflect regional signaling pathway activity rather than necessarily arising from a stem-like cell of origin.

Experimental Procedures

Mice

Generation of the *Pten*$^{loxP/loxP}$ (*LP*) mice has been described previously, and their genetic background was a mixture of 129/Sv, CJ7, and C57BL6/J [37]. Production of the *Ntv-a wt*, *Gtv-a wt*, and *Ntv-a Ink4a-Arf*$^{-/-}$ mouse lines has been described [38]. The resulting genetic backgrounds of *tv-a* transgenic mice were a mixture of FVB/N, C57BL6, BALB/C, and 129. *LP* mice were mated with *tv-a* transgenic mice to produce homozygous *Ntv-a LP*, *Gtv-a LP*, and *Ntv-a Ink4a-Arf*$^{-/-}$ *LP* mice. Screening of *tv-a*, *LP*, and *Ink4a-Arf* alleles has been described [37,38].

RCAS Plasmids

RCAS-*GFPCre* was made by fusing *EGFP* and *Cre* and by cloning the fusion gene into the *Not*1 site of the RCAS-Y vector [62]. We confirmed that the fusion protein expressed from viruses emits fluorescence and can mediate the recombination of *loxP* sites using cultured cell in the presence of a Cre reporter construct CLLA that expresses a floxed *LacZ* followed by alkaline phosphatase (unpublished). RCAS-*LacZ* plasmid was described previously [44]. RCAS-*Akt* carries the activated form of designated Akt-Myr D11-60 and has a *HA* tag sequence added to the 3′ -end of the cDNA. It was a gift from Peter Vogt (The Scripps Research Institute, La Jolla, CA). RCAS-*KRas* (G12D) plasmid was kindly provided by Galen Fisher (Medical University of South Carolina, Charleston, SC).

Infection of Primary Brain Cell Culture

Primary brain cells from newborn *tv-a* transgenic mice were cultured in DMEM with 10% FBS (Gemini) as described before [44]. The supernatants containing various RCAS virons from DF-1 cells transfected with various RCAS plasmids were collected and filtered through 0.22-μm filters, followed by transferring into 70% to 80% confluent primary brain cell cultures. Infections were repeated three times with 12-hour intervals. For selection of primary astrocytes, primary brain cells from *Gtv-a wt* mice were infected with RCAS-*puro* virus and then selected in 4 μg/ml puromycin (Sigma, St. Louis, MO).

Blocking of PI3K and mTOR Signaling in Cell Culture

Selected primary astrocytes were treated with 10 μM LY294002 (stock dissolved in DMSO; Cell Signaling, Beverly, MA) or 10 nM rapamycin (stock dissolved in methanol; Sigma, St. Louis, MO) for 6 days. Fresh medium with the inhibitors was added every 24 hours. After 6 days, two groups of cells treated with inhibitors were cultured in medium without inhibitors for an additional 6 days. The control groups were treated with the same volumes of DMSO and methanol for 6 or 12 days.

PCR Analysis

DNA was extracted from primary *Ntv-a LP* brain cells infected with RCAS viruses or the tail of a *Ntv-a LP*$^{+/-}$ mouse, and subjected to PCR analysis using primer 1 (5′ -AAAAGTTCCCCTGCTGATGATTTGT-3′), primer 2 (5′ -TGTTTTTGACCAATTAAAGTAGGCTGTG-3′), and primer 3 (5′ -CCCCCAAGTCAATTGTTAGGTCTGT-3′). PCR conditions were 95°C, 5 minutes; 95°C, 30 seconds; 55°C, 1 minute; 72°C, 1 minute for 35 cycles using puRe Taq Ready-To-Go PCR Beads (Amersham, Piscataway, NJ).

Western Blot Analysis

Whole cell lysates were dissolved in cold lysis buffer [mammalian protein extraction reagent (M-PER; Pierce, Rockford, IL), 100 mM NaCl, 30 mM NaF, 1mM EDTA, 0.5 mM PMSF, 1 mM Na_3VO_4, and protease inhibitor cocktail tablets (Roche, Indianapolis, IN)] for 30 minutes on ice, followed by centrifugation. Protein concentration was measured by the BCA method (Pierce). Fifty micrograms of protein samples was separated by 10% SDS-PAGE electrophoresis and transferred to PVDF membranes. Membranes were blocked with 5% nonfat milk in phosphate-buffered saline (PBS; pH 7.4) with 0.1% Tween 20. Primary and secondary antibodies were diluted in the same solution. Signals were visualized by ECL chemiluminescence (Amersham) or supersignal chemiluminescence (Pierce). PTEN 1:600 (Cascade, Winchester, MA), P-Akt (Ser473), P-Erk (Ser217/221), Akt and Erk 1:1000 (Cell Signaling), GFAP 1:100 (Santa Cruz Biotechnology, Santa Cruz, CA), GAPDH 1:1000 (Advanced ImmunoChemical, Long Beach, CA), antirabbit HRP 1:1000 (Amersham), and antimouse IgG+IgM HRP and antigoat IgG+IgM HRP 1:1000 (Roche) were used.

Infection of Transgenic Mice

DF-1 cells producing various RCAS virons were trypsinized and pelleted by centrifugation. The pellets were resuspended in approximate 50 μl of medium and placed on ice. Using a 10-μl Hamilton syringe, a single intracranial injection of 1 μl containing 10^4 cells was made in the right frontal region of newborn mice. Statistical analysis was performed with the GraphPad software Prism3 using the log-rank test applied to Kaplan-Meier graphs.

Brain Sectioning, H&E Staining, and Immunohistochemistry

Mice were sacrificed before (due to symptoms of hydrocephalus or lethargy), or at 12 weeks of age. The whole brains were fixed, paraffin-embedded, and processed as previously described [8]. The sections were stained with H&E. As for IHC, slides were stained with primary antibody overnight at 4°C. Immunohistochemistry detection was performed with the ABC kit (Vector Laboratories, Burlingame, CA). PTEN 1:300 (ABM2051; Cascade), HA 1:200 (Y-11; Santa Cruz Biotechnology), P-Erk 1:50 (9101; Cell Signaling), P-S6 1:50 (2211; Cell Signaling), PCNA 1:500 (MAB424R; Chemicon), GFAP 1:1000 (MAB3402; Chemicon, Temecula, CA), nestin 1:200 (556309; PharMingen, San Diego, CA), and Ki-67 1:500 (Novacastra, Newcastle upon Tyne, UK) were used. Olig2 is a gift from John Albeta (Dana-Farber Cancer Institute, Boston, MA).

Treatment of GBM-Bearing Mice

Symptomatic mice were anesthesized with isoflurane and scanned with MRI. For contrast enhancement, mice were intravenously administered 0.2 mM/kg gadolinium diethylenetramine pentaacetic acid. Images were obtained as previously described [41]. Mice with enhancement were treated with CCI-779 (Wyeth, Pearl River, NY) through intraperitoneal injection daily at a dose of 40 mg/kg. The drug was first dissolved to 50 mg/ml in 100% ethanol and then diluted to 2 mg/ml with 5% Tween-80 (Sigma) and 5% polyethylene glycol-400 (Sigma).

Analysis of Olig2-Positive Tumor Cells

The percentage of packed Olig2-positive cell area in the entire untreated and treated GBMs was independently scored by three individuals, followed by averaging the numbers for corresponding GBMs. For each GBM, the average ratio of Olig2-positive cells in the packed area was obtained by counting Olig2-positive and total cells within the tumors in five random microscopic views of 400×. The ultimate percentage of Olig2-positive cells in the tumors was calculated by multiplying the average percentage of packed Olig2-positive cell area and the average percentage of the ratio of Olig2-positive cells. A two-tailed *t*-test was used to evaluate the significance of the difference of Olig2-positive cells between the untreated and 7-day–treated GBMs.

TUNEL Assay

Deparaffinized slides were incubated with 20 μg/ml proteinase K for 20 minutes at room temperature, followed by fixation in 4% paraformaldehyde for 10 minutes at room temperature. Endogenous peroxidase was inactivated by 0.1% hydrogen peroxide in PBS. The sections were incubated with TUNEL dilution buffer (Roche), and then with the same buffer containing biotin-dUTP (Roche) and terminal deoxynucleotidyl transferase (Roche) for 1 hour at 37°C. The reaction was stopped by immersing the slides into 2× SSC (Sigma), and staining was performed using ABC kits (Vector Laboratories).

Acknowledgements

We thank Edward Nerio and Robert J. Finney for histology assistance, and Christina Glaster and Yelena Lyustikman for their help with the preparation of this manuscript. We thank Peter Vogt (The Scripps Research Institute) for the RCAS-*Akt* vector, Galen Fisher (Medical University of South Carolina) for the RCAS-*KRas* (G12D) vector, Jay J. Gibbons (Wyeth) for the CCI-779, and Chuck Stiles and John Albeta (Dana-Farber Cancer Institute) for the Olig2 antibody. Supplemental Materials can be found at: http://www.tgen.org/research/index.cfm?pageid=402.

References

[1] Ueki K, Ono Y, Henson JW, Efird JT, vonDeimling A, and Louis DN (1996). CDKN2/p16 or RB alterations occur in the majority of glioblastomas and are inversely correlated. *Cancer Res* **56,** 150–153.

[2] Wong AJ, Bigner SH, Bigner DD, Kinzler KW, Hamilton SR, and Vogelstein B (1987). Increased expression of the *epidermal growth factor receptor* gene in malignant gliomas is invariably associated with gene amplification. *Proc Natl Acad Sci USA* **84,** 6899–6903.

[3] Fleming TP, Saxena A, Clark WC, Robertson JT, Oldfield EH, Aaronson SA, and Ali IU (1992). Amplification and/or overexpression of platelet-derived growth factor receptors and epidermal growth factor receptor in human glial tumors. *Cancer Res* **52,** 4550–4553.

[4] Wong AJ, Ruppert JM, Bigner SH, Grzeschik CH, Humphrey PA, Bigner DS, and Vogelstein B (1992). Structural alterations of the *epidermal growth factor receptor* gene in human gliomas. *Proc Natl Acad Sci USA* **89,** 2965–2969.

[5] Morrison RS, Yamaguchi F, Saya H, Bruner JM, Yahanda AM, Donehower LA, and Berger M (1994). Basic fibroblast growth factor and fibroblast growth factor receptor I are implicated in the growth of human astrocytomas. *J Neuro-Oncol* **18,** 207–216.

[6] Guha A, Feldkamp MM, Lau N, Boss G, and Pawson A (1997). Proliferation of human malignant astrocytomas is dependent on Ras activation. *Oncogene* **15,** 2755–2765.

[7] Haas-Kogan D, Shalev N, Wong M, Mills G, Yount G, and Stokoe D (1998). Protein kinase B (PKB/Akt) activity is elevated in glioblastoma cells due to mutation of the tumor suppressor PTEN/MMAC. *Curr Biol* **8,** 1195–1198.

[8] Holland EC, Celestino J, Dai C, Schaefer L, Sawaya RE, and Fuller GN (2000). Combined activation of Ras and Akt in neural progenitors induces glioblastoma formation in mice. *Nat Genet* **25,** 55–57.

[9] Li J, Yen C, Liaw D, Podsypanina K, Bose S, Wang SI, Puc J, Miliaresis C, Rodgers L, McCombie R et al. (1997). *PTEN*, a putative protein tyrosine phosphatase gene mutated in human brain, breast, and prostate cancer. *Science* **275,** 1943–1947.

[10] Wang SI, Puc J, Li J, Bruce JN, Cairns P, Sidransky D, and Parsons R (1997). Somatic mutations of PTEN in glioblastoma multiforme. *Cancer Res* **57,** 4183–4186.

[11] Sano T, Lin H, Chen X, Langford LA, Koul D, Bondy ML, Hess KR, Myers JN, Hong YK, Yung WK, et al. (1999). Differential expression of MMAC/PTEN in glioblastoma multiforme: relationship to localization and prognosis. *Cancer Res* **59,** 1820–1824.

[12] Steck PA, Pershouse MA, Jasser SA, Yung WK, Lin H, Ligon AH, Langford LA, Baumgard ML, Hattier T, Davis T, et al. (1997). Identification of a candidate tumour suppressor gene, *MMAC1*, at chromosome 10q23.3 that is mutated in multiple advanced cancers. *Nat Genet* **15,** 356–362.

[13] DiCristofano A, Pesce B, Cordon-Cardo C, and Pandolfi PP (1998). Pten is essential for embryonic development and tumour suppression. *Nat Genet* **19,** 348–355.

[14] Suzuki A, de la Pompa JL, Stambolic V, Elia AJ, Sasaki T, del Barco Barrantes I, Ho A, Wakeham A, Itie A, Khoo W, et al. (1998). High cancer susceptibility and embryonic lethality associated with mutation of the *PTEN* tumor suppressor gene in mice. *Curr Biol* **8,** 1169–1178.

[15] Podsypanina K, Ellenson LH, Nemes A, Gu J, Tamura M, Yamada KM, Cordon-Cardo C, Catoretti G, Fisher PE, and Parsons R (1999). Mutation of Pten/Mmac1 in mice causes neoplasia in multiple organ systems. *Proc Natl Acad Sci USA* **96,** 1563–1568.

[16] Myers MP, Pass I, Batty IH, Van der Kaay J, Stolarov JP, Hemmings BA, Wigler MH, Downes CP, and Tonks NK (1998). The lipid phosphatase activity of PTEN is critical for its tumor suppressor function. *Proc Natl Acad Sci USA* **95,** 13513–13518.

[17] Stambolic V, Suzuki A, de la Pompa JL, Brothers GM, Mirtsos C, Sasaki T, Ruland J, Penninger JM, Siderovski DP, and Mak TW (1998). Negative regulation of PKB/Akt-dependent cell survival by the tumor suppressor PTEN. *Cell* **95,** 29–39.

[18] Stokoe D, Stephens LR, Copeland T, Gaffney PR, Reese CB, Painter GF, Holmes AB, McCormick F, and Hawkins PT (1997). Dual role of phosphatidylinositol-3,4,5-trisphosphate in the activation of protein kinase B. *Science* **277,** 567–570.

[19] Stephens L, Anderson K, Stokoe D, Erdjument-Bromage H, Painter GF, Holmes AB, Gaffney PR, Reese CB, McCormick F, Tempst P, et al. (1998). Protein kinase B kinases that mediate phosphatidylinositol 3,4,5-trisphosphate–dependent activation of protein kinase B. *Science* **279,** 710–714.

[20] Vanhaesebroeck B and Alessi DR (2000). The PI3K-PDK1 connection: more than just a road to PKB. *Biochem J* **3,** 561–576.

[21] Vivanco I and Sawyers CL (2002). The phosphatidylinositol 3-kinase AKT pathway in human cancer. *Nat Rev Cancer* **2,** 489–501.

[22] Inoki K, Li Y, Zhu T, Wu J, and Guan KL (2002). TSC2 is phosphorylated and inhibited by Akt and suppresses mTOR signalling. *Nat Cell Biol* **4,** 648–657.

[23] Garami A, Zwartkruis FJ, Nobukuni T, Joaquin M, Roccio M, Stocker H, Kozma SC, Hafen E, Bos JL, and Thomas G (2003). Insulin activation of Rheb, a mediator of mTOR/S6K/4E-BP signaling, is inhibited by TSC1 and 2. *Mol Cell* **11,** 1457–1466.

[24] Burnett PE, Barrow RK, Cohen NA, Snyder SH, and Sabatini DM (1998). RAFT1 phosphorylation of the translational regulators p70 S6 kinase and 4E-BP1. *Proc Natl Acad Sci USA* **95,** 1432–1437.

[25] Volarevic S and Thomas G (2001). Role of S6 phosphorylation and S6 kinase in cell growth. *Prog Nucleic Acid Res Mol Biol* **65,** 101–127.

[26] Gingras AC, Raught B, and Sonenberg N (2001). Regulation of translation initiation by FRAP/mTOR. *Genes Dev* **15,** 807–826.

[27] Rajasekhar VK, Viale A, Socci ND, Wiedmann M, Hu X, and Holland EC (2003). Oncogenic Ras and Akt signaling contribute to glioblastoma formation by differential recruitment of existing mRNAs to polysomes. *Mol Cell* **12,** 889–901.

[28] Neshat MS, Mellinghoff IK, Tran C, Stiles B, Thomas G, Petersen R, Frost P, Gibbons JJ, Wu H, and Sawyers CL (2001). Enhanced sensitivity of PTEN-deficient tumors to inhibition of FRAP/mTOR. *Proc Natl Acad Sci USA* **98,** 10314–10319.

[29] Podsypanina K, Lee RT, Politis C, Hennessy I, Crane A, Puc J, Neshat M, Wang H, Yang L, Gibbons J, et al. (2001). An inhibitor of mTOR reduces neoplasia and normalizes p70/S6 kinase activity in Pten$^{+/-}$ mice. *Proc Natl Acad Sci USA* **98,** 10320–10325.

[30] Aoki M, Blazek E, and Vogt PK (2001). A role of the kinase mTOR in cellular transformation induced by the oncoproteins P3k and Akt. *Proc Natl Acad Sci USA* **98,** 136–141.

[31] Choe G, Horvath S, Cloughesy TF, Crosby K, Seligson D, Palotie A, Inge L, Smith BL, Sawyers CL, and Mischel PS (2003). Analysis of the phosphatidylinositol 3′ -kinase signaling pathway in glioblastoma patients *in vivo*. *Cancer Res* **63,** 2742–2746.

[32] Uhrbom L, Dai C, Celestino JC, Rosenblum MK, Fuller GN, and Holland EC (2002). Ink4a-Arf loss cooperates with KRas activation in astrocytes and neural progenitors to generate glioblastomas of various morphologies depending on activated Akt. *Cancer Res* **62,** 5551–5558.

[33] Dai C, Shih A, Lyustikman Y, Hu X, Fuller GN, Rosenblum MK, and Holland EC (2004). The characteristics of astrocytomas and oligodendrogliomas are caused by two distinct and interchangeable signaling formats. Neoplasia (In press).

[34] Tamura M, Gu J, Matsumoto K, Aota S, Parsons R, and Yamada KM (1998). Inhibition of cell migration, spreading, and focal adhesions by tumor suppressor PTEN. *Science* **280,** 1614–1617.

[35] Gu J, Tamura M, Pankov R, Danen EH, Takino T, Matsumoto K, and Yamada KM (1999). Shc and FAK differentially regulate cell motility and directionality modulated by PTEN. *J Cell Biol* **146,** 389–403.

[36] Weng LP, Smith WM, Brown JL, and Eng C (2001). PTEN inhibits insulin-stimulated MEK/MAPK activation and cell growth by blocking IRS-1 phosphorylation and IRS-1/Grb-2/Sos complex formation in a breast cancer model. *Hum Mol Genet* **10,** 605–616.

[37] Trotman LC, Niki M, Dotan ZA, Koutcher JA, Cristofano AD, Xiao A, Khoo AS, Roy-Burman P, Greenberg NM, Dyke TV, et al. (2003). Pten dose dictates cancer progression in the prostate. *PLoS Biol* **1,** E59.

[38] Holland EC, Hively WP, DePinho RA, and Varmus HE (1998). A constitutively active epidermal growth factor receptor cooperates with disruption of G1 cell-cycle arrest pathways to induce glioma-like lesions in mice. *Genes Dev* **12,** 3675–3685.

[39] Holland EC and Varmus HE (1998). Basic fibroblast growth factor induces cell migration and proliferation after glia-specific gene transfer in mice. *Proc Natl Acad Sci USA* **95,** 1218–1223.

[40] Loonstra A, Vooijs M, Beverloo HB, Allak BA, van Drunen E, Kanaar R, Berns A, and Jonkers J (2001). Growth inhibition and DNA damage induced by Cre recombinase in mammalian cells. *Proc Natl Acad Sci USA* **98,** 9209–9214.

[41] Koutcher JA, Hu X, Xu S, Gade TP, Leeds N, Zhou XJ, Zagzag D, and Holland EC (2002). MRI of mouse models for gliomas shows similarities to humans and can be used to identify mice for preclinical trials. *Neoplasia* **4,** 480–485.

[42] Kwon CH, Zhu X, Zhang J, Knoop LL, Tharp R, Smeyne RJ, Eberhart CG, Burger PC, and Baker SJ (2001). Pten regulates neuronal soma size: a mouse model of Lhermitte-Duclos disease. *Nat Genet* **29,** 404–411.

[43] Tascos NA, Parr J, and Gonatas NK (1982). Immunocytochemical study of the glial fibrillary acidic protein in human neoplasms of the central nervous system. *Hum Pathol* **13,** 454–458.

[44] Dai C, Celestino JC, Okada Y, Louis DN, Fuller GN, and Holland EC (2001). PDGF autocrine stimulation dedifferentiates cultured astrocytes and induces oligodendrogliomas and oligoastrocytomas from neural progenitors and astrocytes *in vivo*. *Genes Dev* **15,** 1913–1925.

[45] Marie Y, Sanson M, Mokhtari K, Leuraud P, Kujas M, Delattre JY, Poirier J, Zalc B, and Hoang-Xuan K (2001). OLIG2 as a specific marker of oligodendroglial tumour cells. *Lancet* **358,** 298–300.

[46] Ligon KL, Alberta JA, Kho AT, Weiss J, Kwaan MR, Nutt CL, Louis DN, Stiles CD, and Rowitch DH (2004). The oligodendroglial lineage marker OLIG2 is universally expressed in diffuse gliomas. *J Neuropathol Exp Neurol* **63,** 499–509.

[47] Kleihues P, Cavenee WK, et al. (2000). Pathology and Genetics of Tumours of the Nervous System Lyon, IARC Press.

[48] Backman SA, Stambolic V, Suzuki A, Haight J, Elia A, Pretorius J, Tsao MS, Shannon P, Bolon B, Ivy GO, et al. (2001). Deletion of Pten in mouse brain causes seizures, ataxia and defects in soma size resembling Lhermitte-Duclos disease. *Nat Genet* **29,** 396–403.

[49] Groszer M, Erickson R, Scripture-Adams DD, Lesche R, Trumpp A, Zack JA, Kornblum HI, Liu X, and Wu H (2001). Negative regulation of neural stem/progenitor cell proliferation by the *Pten* tumor suppressor gene *in vivo*. *Science* **294,** 2186–2189.

[50] Kwon CH, Zhu X, Zhang J, and Baker SJ (2003). mTOR is required for hypertrophy of Pten-deficient neuronal soma *in vivo*. *Proc Natl Acad Sci USA* **100,** 12923–12928.

[51] Maier D, Jones G, Li X, Schonthal AH, Gratzl O, Van Meir EG, and Merlo A (1999). The PTEN lipid phosphatase domain is not required to inhibit invasion of glioma cells. *Cancer Res* **59,** 5479–5482.

[52] Freeman DJ, Li AG, Wei G, Li HH, Kertesz N, Lesche R, Whale AD, Martinez-Diaz H, Rozengurt N, Cardiff RD, et al. (2003). PTEN tumor suppressor regulates p53 protein levels and activity through phosphatase-dependent and -independent mechanisms. *Cancer Cell* **3,** 117–130.

[53] Knobbe CB, Merlo A, and Reifenberger G (2002). Pten signaling in gliomas. *Neuro-Oncology* **4,** 196–211.

[54] Schmelzle T and Hall MN (2000). TOR, a central controller of cell growth. *Cell* **103,** 253–262.

[55] Castedo M, Ferri KF, and Kroemer G (2002). Mammalian target of rapamycin (mTOR): pro- and anti-apoptotic. *Cell Death Differ* **9,** 99–100.

[56] Dennis PB, Jaeschke A, Saitoh M, Fowler B, Kozma SC, and Thomas G (2001). Mammalian TOR: a homeostatic ATP sensor. *Science* **294,** 1102–1105.

[57] Majumder PK, Febbo PG, Bikoff R, Berger R, Xue Q, McMahon LM, Manola J, Brugarolas J, McDonnell TJ, Golub TR, et al. (2004). mTOR inhibition reverses Akt-dependent prostate intraepithelial neoplasia through regulation of apoptotic and HIF-1–dependent pathways. *Nat Med* **10,** 594–601.

[58] Wendel HG, De Stanchina E, Fridman JS, Malina A, Ray S, Kogan S, Cordon-Cardo C, Pelletier J, and Lowe SW (2004). Survival signalling by Akt and eIF4E in oncogenesis and cancer therapy. *Nature* **428,** 332–337.

[59] Ignatova TN, Kukekov VG, Laywell ED, Suslov ON, Vrionis FD, and Steindler DA (2002). Human cortical glial tumors contain neural stem–like cells expressing astroglial and neuronal markers *in vitro*. *Glia* **39,** 193–206.

[60] Hemmati HD, Nakano I, Lazareff JA, Masterman-Smith M, Geschwind DH, Bronner-Fraser M, and Kornblum HI (2003). Cancerous stem cells can arise from pediatric brain tumors. *Proc Natl Acad Sci USA* **100,** 15178–15183.

[61] Singh SK, Clarke ID, Terasaki M, Bonn VE, Hawkins C, Squire J, and Dirks PB (2003). Identification of a cancer stem cell in human brain tumors. *Cancer Res* **63,** 5821–5828.

[62] Dunn KJ, Williams BO, Li Y, and Pavan WJ (2000). Neural crest–directed gene transfer demonstrates Wnt1 role in melanocyte expansion and differentiation during mouse development. *Proc Natl Acad Sci USA* **97,** 10050–10055.